Available online at www.sciencedirect.com
ScienceDirect
Journal of Electrostatics 65 (2007) 322–328
Journal of ELECTROSTATICS
www.elsevier.com/locate/elstat

Lightning-induced currents in buried coaxial cables: A frequency-domain approach and its validation using rocket-triggered lightning

E. Petrache[a], M. Paolone[b], F. Rachidi[c,*], C.A. Nucci[b], V. Rakov[d], M. Uman[d], D. Jordan[d], K. Rambo[d], J. Jerauld[d], M. Nyffeler[e], J. Schoene[d]

[a]Department of Electrical and Computer Engineering, University of Toronto, Toronto, Canada
[b]Department of Electrical Engineering, University of Bologna, Bologna, Italy
[c]Power Systems Laboratory, Swiss Federal Institute of Technology, EMC Group, Lausanne, Switzerland
[d]Department of Electrical and Computer Engineering, University of Florida, Gainesville, FL, USA
[e]Armasuisse, NEMP Labor, Spiez, Switzerland

Received 13 September 2004; accepted 13 September 2006
Available online 13 November 2006

Abstract

The aim of this paper is to present an experimental validation of a frequency-domain approach to the solution of the lightning electromagnetic field-to-buried cable coupling equations. The coupling to the inner conductor is evaluated using the concept of cable transfer impedance. The theoretical model and relevant computer code are tested using experimental data on lightning-induced currents in buried cables carried out in 2002 and 2003 at the International Center for Lightning Research & Testing (ICLRT) at Camp Blanding, Florida where currents induced by triggered lightning events were measured at the ends of a buried coaxial cable, both in the shield and in the inner cable conductors. Reasonably good agreement has been found between numerical simulations and recorded waveforms. In particular, the early-time response of the cable and the peak value of the induced currents were generally well reproduced by the simulations.

Keywords: Lightning; Induced currents; Buried cables; Coaxial cables; LEMP-to-buried cables electromagnetic coupling

1. Introduction

Experimental results on lightning-induced disturbances in buried cables have recently been obtained at the International Center for Lightning Research & Testing (ICLRT) at Camp Blanding, Florida, where, during 2002 and 2003, currents induced by triggered lightning were measured at both ends of a buried coaxial power cable, both in the shield and in the inner conductor [1–3]. Simultaneously, the horizontal magnetic field and the return stroke current at the triggered-lightning channel base were also measured. The obtained experimental data have been used to test theoretical models and computer codes developed for the calculation of lightning-induced currents in buried cables [2]. In this paper, we extend the analysis presented in [2,3] by considering also the coupling to the inner conductor of the buried coaxial cable using a frequency-domain approach. The mechanism of coupling through the cable shield is described using the concept of transfer impedance [4].

2. Computation of lightning-induced disturbances in buried shielded cables

A frequency-domain solution is particularly useful when one is interested in calculating the inner conductor response of a coaxial cable. In this case, the external fields can penetrate through the imperfections of the cable sheath—a process that is highly frequency dependent—producing induced currents and voltages on the inner conductor.

*Corresponding author. Fax: +41 21 693 46 62.
E-mail address: farhad.rachidi@epfl.ch (F. Rachidi).

0304-3886/$ - see front matter © 2006 Elsevier B.V. All rights reserved.
doi:10.1016/j.elstat.2006.09.015

The problem under study can be divided in two different transmission line problems [4]. One is the "external" problem in which the illuminating field serves as the excitation and the line is composed of the cable shield with the ground as the return conductor. The other problem involves the internal transmission line geometry, in which the excitation arises from the penetration of the field through the cable shield and the response is the resulting current in the inner conductor and the induced voltage between the inner conductor and the shield.

2.1. External coupling to the cable shield

Consider a horizontal buried cable of length L (cylindrical conductor representing the cable shield with the relevant insulating jacket) located along the x-axis at depth d. Assuming that the vertical component of electric field can be neglected below the ground surface [5], voltages and currents along the cable induced by a nearby lightning can be calculated using the field-to-transmission line equations expressed in the frequency-domain [2,4,6,7]:

$$\frac{dV_e(x)}{dx} + (j\omega L' + Z'_w + Z'_g)I_e(x) = E^e_x(x, z = -d), \tag{1}$$

$$\frac{dI_e(x)}{dx} + \frac{(G + j\omega C')Y'_g}{(G + j\omega C') + Y'_g} V_e(x) = 0, \tag{2}$$

in which V_e and I_e are the voltage and current of the shield; $E^e_x(x, z = -d)$ is the horizontal component of the incident electric field generated by the lightning discharge parallel to the cable; L', G' and C' are, respectively the per-unit-length longitudinal inductance, transverse conductance and transverse capacitance of the cable, Z'_w is the per-unit-length internal impedance of the conductor (wire), Z'_g and Y'_g are the per-unit-length ground impedance and ground admittance. Expressions for the line parameters can be found in [2].

One method to solve the field-to-transmission line (Eqs. (1) and (2)) in the frequency domain is to use the expression for the line voltage and current for a point voltage source and a current point source, respectively, namely the Green's functions. For an arbitrary incident field exciting the cable (vertical electric field component in the ground is neglected), the solution for the cable current and voltage at an arbitrary position x on the cable can be written as the following integrals of the Green's functions [4]:

$$I_e(x) = \int_0^L G_I(x, x_s) E^e_x(x_s, z = -d)\, dx_s, \tag{3}$$

$$V_e(x) = \int_0^L G_V(x, x_s) E^e_x(x_s, z = -d)\, dx_s, \tag{4}$$

where G_I and G_V represent the Green's function for the cable current and voltage, respectively, which are given by Tesche et al. [4]:

$$G_I(x, x_s) = \begin{cases} \frac{e^{-\gamma L}}{2Z_c(1-\rho_1\rho_2 e^{-2\gamma L})}\left[e^{-\gamma(x_s - L)} - \rho_2 e^{\gamma(x_s - L)}\right] \\ \quad \times \left(e^{\gamma x} - \rho_1 e^{-\gamma x}\right) \quad \text{for } x < x_s, \\ \frac{e^{-\gamma L}}{2Z_c(1-\rho_1\rho_2 e^{-2\gamma L})}\left[e^{-\gamma(x - L)} - \rho_2 e^{\gamma(x - L)}\right] \\ \quad \times \left(e^{\gamma x_s} - \rho_1 e^{-\gamma x_s}\right) \quad \text{for } x > x_s, \end{cases} \tag{5}$$

$$G_V(x, x_s) = \begin{cases} \frac{-e^{-\gamma L}}{2(1-\rho_1\rho_2 e^{-2\gamma L})}\left[e^{-\gamma(x_s - L)} - \rho_2 e^{\gamma(x_s - L)}\right] \\ \quad \times \left(e^{\gamma x} + \rho_1 e^{-\gamma x}\right) \quad \text{for } x < x_s, \\ \frac{e^{-\gamma L}}{2(1-\rho_1\rho_2 e^{-2\gamma L})}\left[e^{-\gamma(x - L)} + \rho_2 e^{\gamma(x - L)}\right] \\ \quad \times \left(e^{\gamma x_s} - \rho_1 e^{-\gamma x_s}\right) \quad \text{for } x > x_s, \end{cases} \tag{6}$$

where $\gamma = \sqrt{Z'Y'}$ is the line complex propagation constant along the cable and $Z_c = \sqrt{Z'/Y'}$ is the cable characteristic impedance.

2.2. Internal coupling to the inner conductor

The coupling to the internal circuit formed by the inner conductor and the cable shield can be expressed in the frequency domain as [4]

$$\frac{dV_i(x)}{dx} + Z'_i I_i(x) = Z'_t I_e(x), \tag{7}$$

$$\frac{dI_i(x)}{dx} + Y'_i V_i(x) = -Y'_t V_e(x), \tag{8}$$

where V_i and I_i are the voltage and current of the inner conductor, Z'_i, Y'_i are the per-unit-length longitudinal impedance and transverse admittance of the internal coupling circuit, and, Z'_t, Y'_t are the transfer impedance and the transfer admittance characterizing the field penetration through the cable shield [4].

Note that it is implicitly assumed that the external circuit, composed by the cable shield and ground, has an independent behavior from the internal circuit. For the frequencies of interest (e.g. not exceeding 10 MHz or so), the contribution of the transfer admittance is generally small compared to that of the transfer impedance, and therefore, can be neglected in the calculations [4].

The internal coupling equations can be solved in a way similar to that followed for the external coupling case, using the Green's functions:

$$I_i(x) = \int_0^L G_{I_i}(x, x_s) Z'_t I_e(x_s)\, dx_s, \tag{9}$$

$$V_i(x) = \int_0^L G_{V_i}(x, x_s) Z'_t I_e(x_s)\, dx_s, \tag{10}$$

where G_{I_i} and G_{V_i} represent, respectively, the Green's functions for the cable inner current and voltage, which are given in (5) and (6) with: $\gamma = \gamma_i = \sqrt{Z'_i Y'_i}$ line complex propagation constant along the inner conductor; $Z_c = Z_{ci} = \sqrt{Z'_i/Y'_i}$ line characteristic impedance for the inner conductor.

3. Experimental cable transfer impedance

The underground cable considered here is a 15-kV XLPE coaxial power cable, 133-m long, covered with an insulating jacket. The geometrical characteristics of the cable can be found in [3].

Given the inhomogeneous nature of the braided shield and the complexity of the electromagnetic field penetration into the cable, the reliable method for determining the transfer impedance is by measurement [4]. The transfer impedance of the cable was measured at the EMC laboratory of the Swiss Federal Institute of Technology in Lausanne using a triaxial-adapted measurement set up [8]. The results are presented in Fig. 1.

4. Experimental setup

The topology of the experimental setup is shown in Fig. 2. The triggering rockets were launched using a mobile launcher, placed at different positions, as indicated in Fig. 2. The channel base current was measured using a 1.25 mΩ coaxial shunt (T&M Research Products, Inc., model R-5600-8) having a bandwidth of DC to 12 MHz. Fiber optic links, with a 15 MHz bandwidth, were employed to relay the signals to the digitizer.

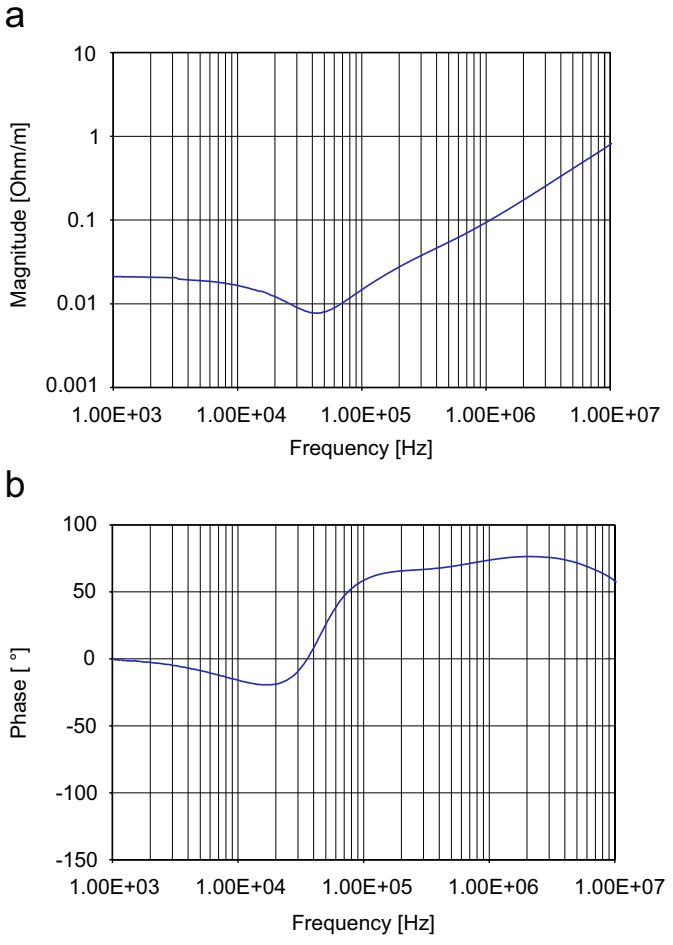

Fig. 1. Transfer impedance of the coaxial cable: (a) magnitude; (b) phase (adapted from [3]).

The terminations of the cable were placed inside metallic boxes located in two instrument stations (IS1 and IS2) as illustrated in Fig. 2 in which the inner conductor was terminated at each end with a 50 Ω resistor, a value close to the surge impedance of the cable (about 58 Ω). The shield of the cable was connected directly to vertical ground electrodes at each of its extremities. The ground electrodes were cylindrical vertical rods of 12 m (IS1) and 24 m (IS2) in length, respectively. The measured value of DC grounding resistance was 60 Ω for the ground electrode of IS1 and 37 Ω for the one of IS2. The conductivity of the soil was determined from the measurements of the grounding resistance of the electrodes and their geometry to be in the range 1.6×10^{-3} to 1.8×10^{-3} S/m.

During the summer of 2002, both triggered and natural lightning events were recorded. Simultaneous measurements of lightning return stroke current (in the case of triggered lightning), horizontal magnetic field (perpendicular to the cable), and currents induced in the shield and in the inner conductor of the cable at the IS2 termination were obtained [1,3].

During the summer of 2003, more experimental data were gathered using the same experimental setup and for additional strike locations. Moreover, lightning-induced currents were recorded at both ends of the cable.

Fig. 2 shows three triggered events (stroke locations 1–3) for which experimental data were recorded.

The magnetic field was measured using a magnetic field sensor (TSN 245-H32, Thomson CSF) located at two different positions shown in Fig. 2 and having a bandwidth of 1 kHz to 130 MHz.

The induced currents were measured using the following sensors: for the inner conductor, Eaton 112 current transformers with a bandwidth of 10 kHz to 200 MHz were used during the 2002 experiments and Pearson 410 current transformers with a bandwidth of 1 Hz to 20 MHz in 2003. For the shield, Pearson 110 current transformers with a bandwidth of 1 Hz to 20 MHz were used both in 2002 and 2003.

The measured signals from all the sensors were relayed via optical fiber links to an 8-bit digitizing oscilloscope operating at 100 MS/s. The digitizer features a segmented memory (1 Mbyte per 4 channels) which is used to record waveshapes for up to 10 strokes per lightning flash with a time window of 100 μs per stroke.

5. Numerical simulations and comparison with experimental waveforms

During experimental campaigns in 2002 and 2003, a total number of 15 flashes with 42 strokes were recorded. A more detailed analysis of the experimental data can be found in [3]. We use in this study three sets of typical

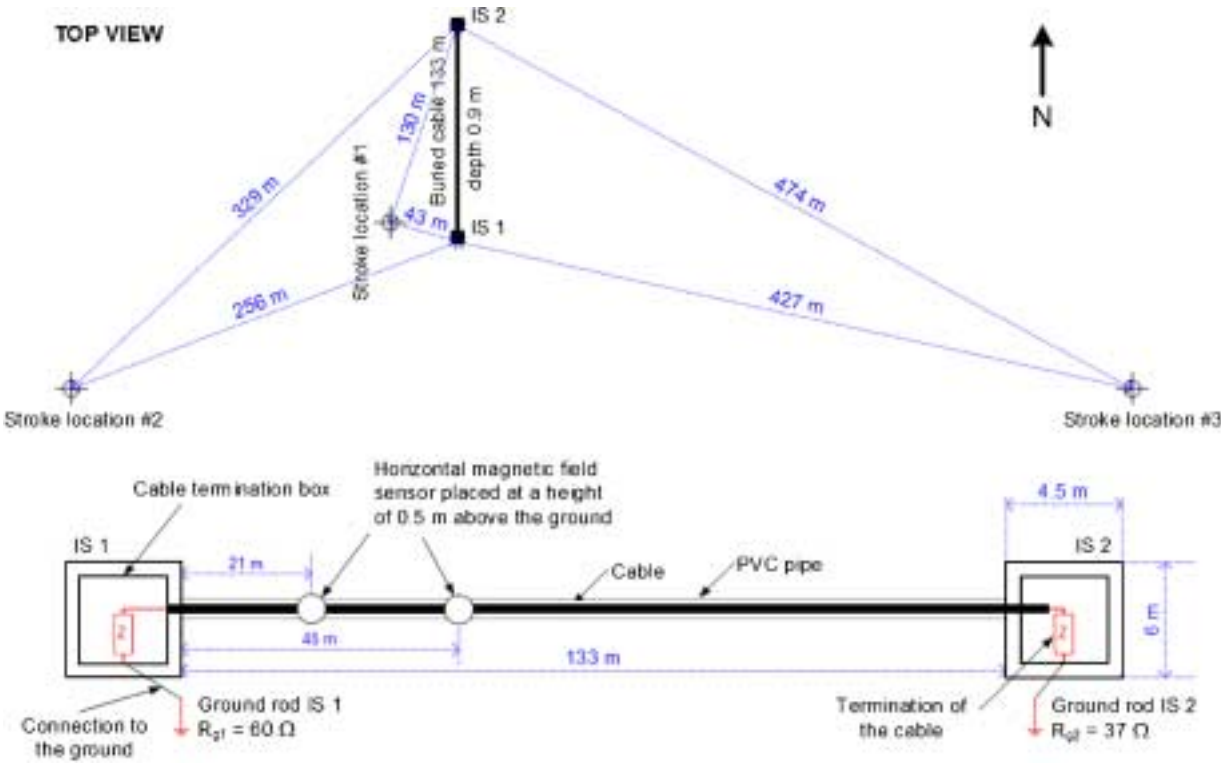

Fig. 2. Buried cable experimental setup and the positions of the lightning strokes analyzed in this paper (adapted from [3]).

experimental data obtained for stroke locations #1, #2 and #3, shown in Fig. 2.

The calculation has been performed adopting for the spatial-temporal distribution of the lightning current, the MTLE model [9,10] and assuming an exponential decay constant $\lambda = 2\,\mathrm{km}$ and a return stroke speed $v = 1.3 \times 10^8\,\mathrm{m/s}$. Note that the initial part (between -10 and $0\,\mu\mathrm{s}$) of the measured magnetic field waveform is due to the leader phase and, hence, it is not reproduced by the return-stroke model. The electric field in the ground along the cable has been evaluated using the Cooray expression [2,5]. The channel-base current waveforms have been represented using the so-called Heidler's functions whose parameters were determined using the genetic algorithm described in [11].

Concerning the modeling of the vertical grounding rods connected at both ends to the cable shield, a circuit-model approach, illustrated in Fig. 3, is used. In particular, a discrete approximation of a distributed-parameter circuit was adopted by dividing the rod into N segments, each one represented by a R-L-C section [12].

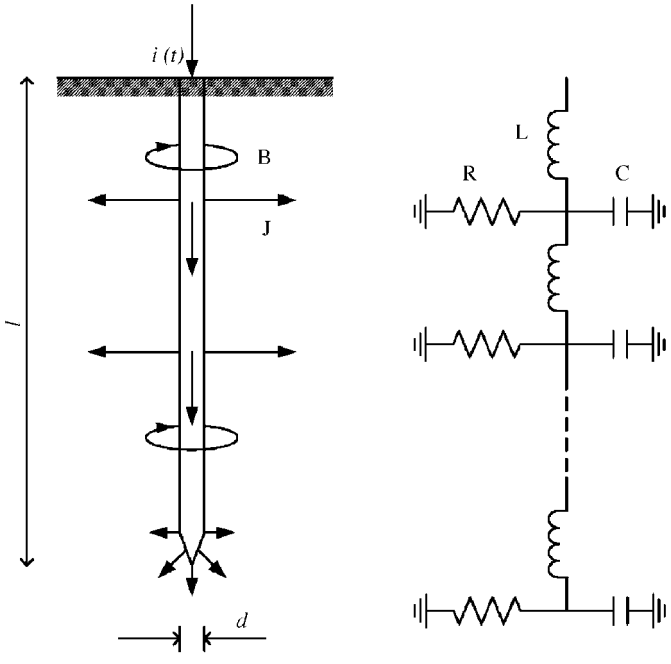

Fig. 3. Lumped parameter representation of the vertical grounding rods.

5.1. Strike location #1 (recorded on August 18, 2002), 1st return stroke

Measured currents in the cable shield and in the inner conductor at the IS2 termination, and the numerical simulations are presented in Figs. 4 and 5, respectively. It can be seen that the simulation results are in very good agreement with experimental data. For this case, from the 2002 experiments, no measured currents at IS1 are available.

5.2. Strike location #2 (recorded on July 22, 2003), 3rd return stroke

Fig. 6 presents the experimental data and the simulation results for lightning-induced currents in the shield of the experimental cable for the strike location #2 (see Fig. 2). The results are given for the observation points located at both terminations of the experimental cable. It can be seen that the simulations are in reasonable agreement with experimental data. In particular, the early-time response of the cable and the peak value of the induced current are very well reproduced by the simulations (Figs. 6 and 7).

Noticeable differences appear, however, for the late-time response. These disagreements can be attributed to simplifying assumptions of the model, uncertainties in the knowledge of the ground electrical parameters and their possible non-homogeneities, as well as in the representation of the ground rods [3]. In addition, the cable shield was connected to the ground rods using a metallic strap, introducing an additional impedance. Finally, at both ends of the buried cable, a vertical portion of the cable

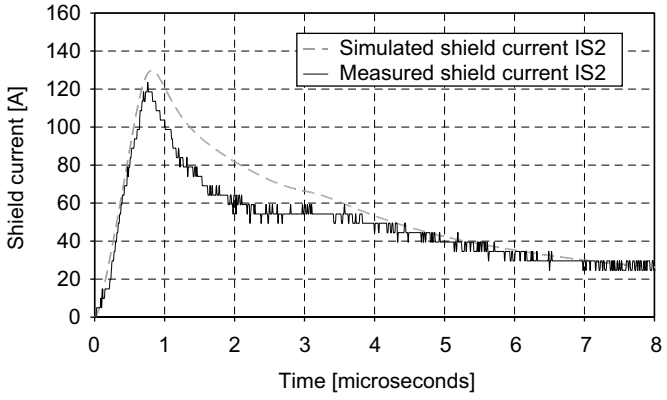

Fig. 4. Experimental data and simulation results for the lightning-induced currents in the shield of the experimental cable for the first return stroke of a single stroke flash recorded on August 18, 2002; strike location #1 (see Fig. 2).

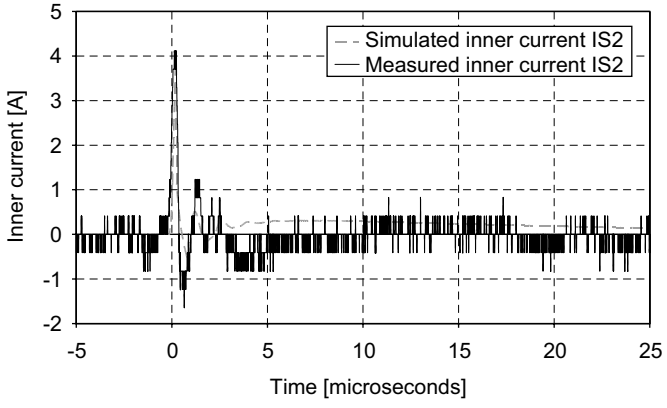

Fig. 5. Experimental data and simulation results for the lightning-induced currents in the inner conductor of the experimental cable for the flash recorded on August 18, 2002; strike location #1 (see Fig. 2).

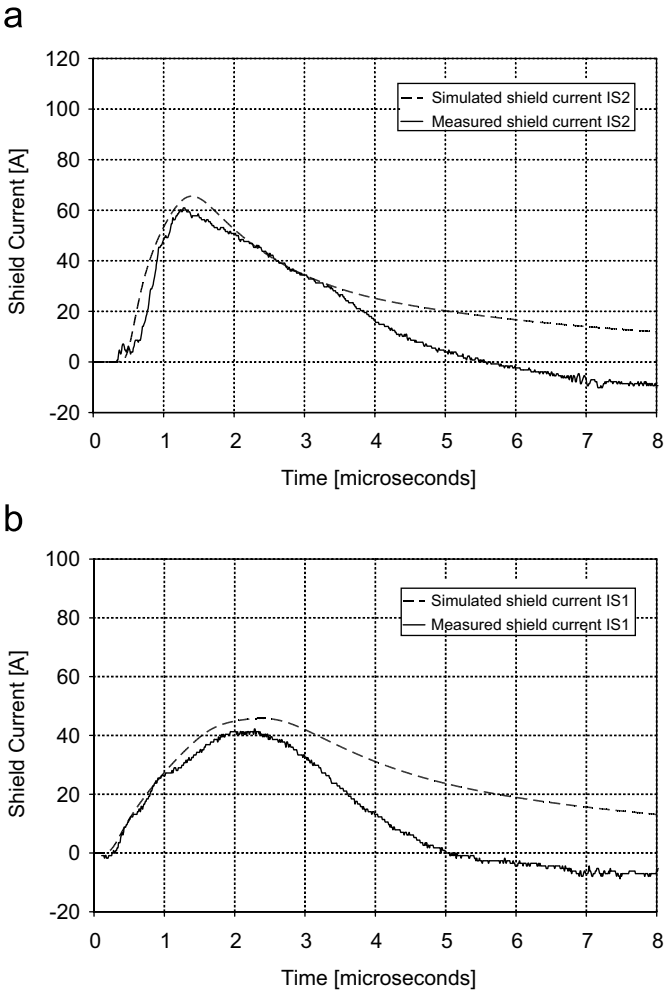

Fig. 6. Experimental data and simulation results for the lightning-induced currents in the shield of the experimental cable for the third return stroke of a four-stroke flash recorded on July 22, 2003; strike location #2 (see Fig. 2).

(about 2 m) was located above ground (up to the termination boxes). Although the vertical part of the cable was shielded using meshed screen to minimize the electromagnetic field coupling to it [3], a contribution from a direct coupling to these vertical cable sections cannot be totally ruled out.

Fig. 7 presents a comparison between the current induced in the inner conductor of the experimental coaxial buried cable and its simulation for the same stroke location #2. It can be seen that the simulations are in good agreement with experimental data, especially at the early times.

5.3. Strike location #3 (recorded on August 15, 2003), 1st return stroke

Measured and computed shield currents for the event recorded on August 15, 2003, strike location #3, are presented in Figs. 8. For this case, the agreement between measured and simulated waveforms is less satisfactory compared to the two other cases corresponding to strike

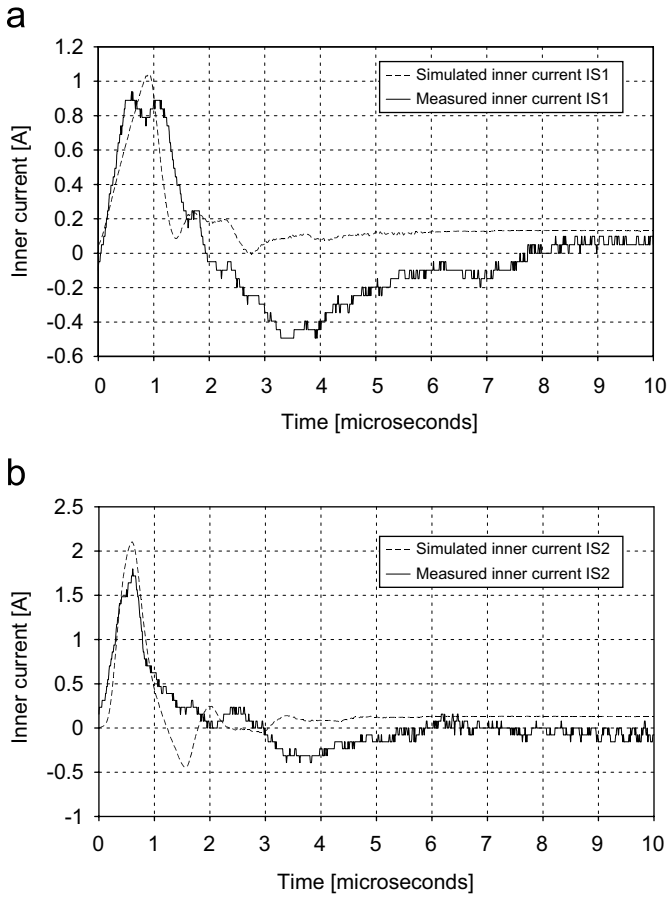

Fig. 7. Experimental data and simulation results for the lightning-induced currents in the inner conductor of the experimental cable for the third return stroke of a four-stroke flash recorded on July 22, 2003; stroke location #2 represented in the Fig. 2.

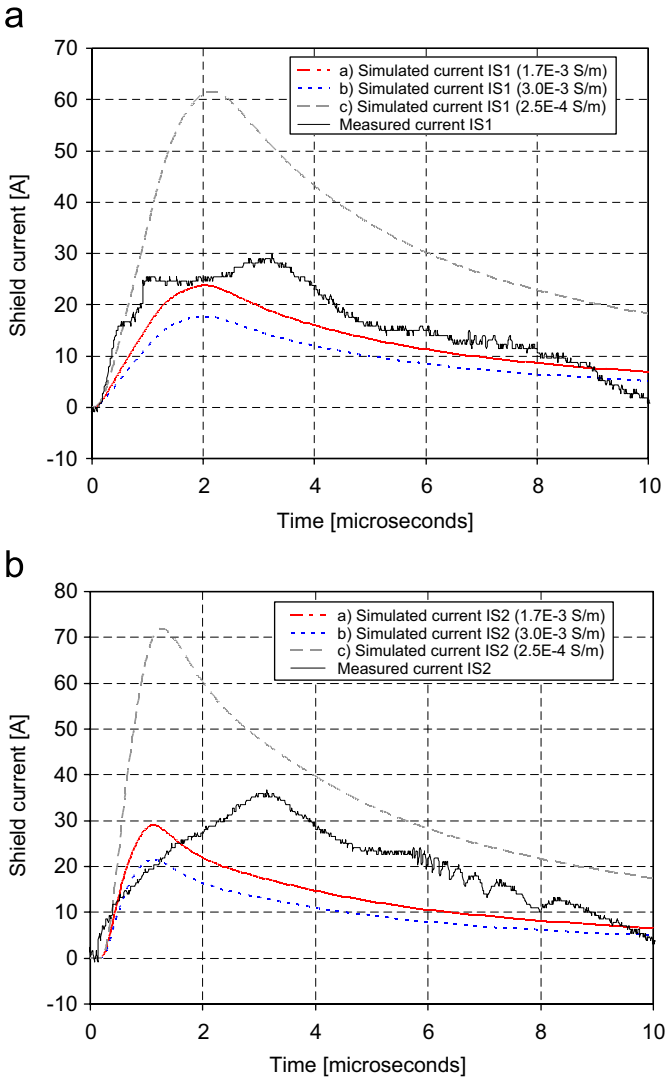

Fig. 8. Experimental data and simulation results for the lightning-induced currents in the shield of the experimental cable for the first return stroke of the flash recorded on August 15, 2003; strike location #3 (see Fig. 2). The computations have been performed for different ground conductivities: (a) 1.7×10^{-3} S/m, (b) 3×10^{-3} S/m and (c) 2.5×10^{-4} S/m.

locations #1 and #2. As discussed in [3], the observed discrepancies for this case can be partially explained by the fact that the propagation path from the strike location #3 to the cable was longer than for the other strike locations, and included extensive swampy soil regions. In the same figure, we have reproduced simulation results obtained assuming different values for the ground conductivity, namely (a) 1.7×10^{-3} S/m, (b) 3×10^{-3} S/m and (c) 2.5×10^{-4} S/m. It can be seen that for a conductivity of the soil of 1.7×10^{-3} S/m, we obtain a better agreement with experimental data [3].

Figs. 9 presents the measured and computed results (obtained with $\sigma_g = 1.7 \times 10^{-3}$ S/m) for the current in the inner conductor. Although the differences between calculated and measured waveforms are smaller compared to the currents in the shield, the agreement is less satisfactory than in the previous cases.

6. Conclusion

Experiments on lightning-induced currents in buried cables have been carried out in 2002 and 2003 at the International Center for Lightning Research & Testing (ICLRT) at Camp Blanding, Florida, where currents induced by triggered lightning events were measured at the ends of a buried coaxial cable, both in the shield and in the inner conductor.

We present in this paper a frequency-domain approach to solve the field-to-buried cable coupling equations. The coupling to the inner conductor is evaluated using the concept of cable transfer impedance. The obtained experimental data are then used to test the validity of the numerical simulations provided by the relevant developed codes.

In general, reasonably good agreement has been found between numerical simulations and recorded waveforms. In particular, the early-time response of the cable and the peak value of the induced currents were generally well reproduced by the simulations. We believe the main cause

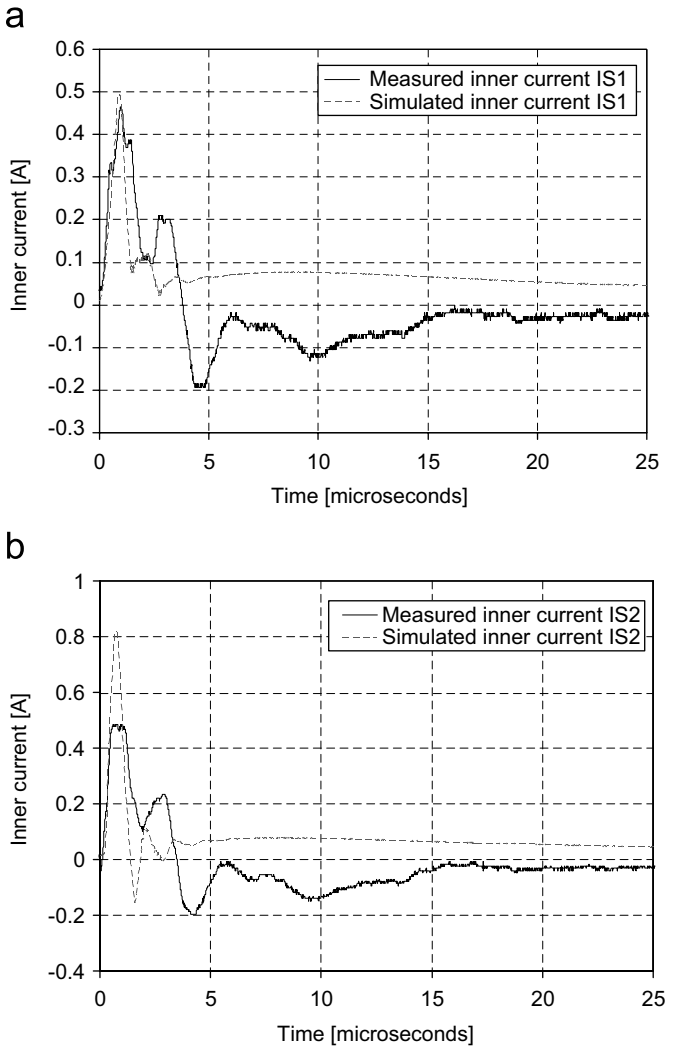

Fig. 9. Experimental data and simulation results for the lightning-induced currents in the inner conductor of the experimental cable for the flash recorded on 15 August, 2003; stroke location #3 represented in Fig. 2; $\sigma_g = 1.7 \times 10^{-3}$ S/m.

of the observed disagreement related to uncertainties in the knowledge of the ground electrical parameters and their possible non-homogeneities.

Acknowledgments

This work was supported in part by Alcatel Submarine Network Division, Armasuisse and by NSF grants ATM 0003994 and ATM 0346164.

References

[1] E. Petrache, M. Paolone, F. Rachidi, C.A. Nucci, V.A. Rakov, M.A. Uman, D. Jordan, K. Rambo, J. Schoene, A. Cordier, T. Verhaege, Measurement of lightning-induced currents in an experimental coaxial buried cable, presented at IEEE Power Engineering Society Summer Meeting, Toronto, Canada, 2003.

[2] E. Petrache, F. Rachidi, M. Paolone, C. Nucci, V.A. Rakov, M.A. Uman, Lightning-induced voltages on buried cables, Part I: Theory, IEEE Trans. Electromagn. Compatibility 47-3 (2005) 498–508.

[3] M. Paolone, E. Petrache, F. Rachidi, C.A. Nucci, V.A. Rakov, M.A. Uman, D. Jordan, K. Rambo, J. Jerauld, M. Nyffeler, J. Schoene, Lightning-induced voltages on buried cables. Part II: Experiment and model validation,, IEEE Trans. Electromagn. Compatibility 47-3 (2005) 509–520.

[4] F.M. Tesche, M. Ianoz, T. Karlsson, EMC Ananlysis Methods and Computational Models, Wiley Interscience, New York, 1997.

[5] V. Cooray, Underground electromagnetic fields generated by the return strokes of lightning flashes, IEEE Trans. Electromagn. Compatibility 43 (2001) 75–84.

[6] A. Galvan, V. Cooray, Lightning induced voltages on bare and insulated buried cables, presented at 13th Zurich International Symposium on EMC, Zurich, Switzerland, 1999.

[7] E.F. Vance, Coupling with Shielded Cables, Wiley, New York, 1978.

[8] P. Degauque, J. Hamelin, Compatibilité électromagnétique, Dunod, Paris, France, 1990.

[9] C. A. Nucci, C. Mazzetti, F. Rachidi, M. Ianoz, On lightning return stroke models for LEMP calculations, presented at 19th International Conference on Lightning Protection, Graz, 1988.

[10] F. Rachidi, C.A. Nucci, On the Master, Uman, Lin, Standler and the Modified Transmission Line lightning return stroke current models,, J. Geophys. Res. 95 (1990) 20389–20394.

[11] J.L. Bermudez, C.A. Pena, F. Rachidi, F. Heidler, V. A. Rakov, Analytical representation of lightning current waveforms using genetic algorithms, presented at International Conference on Lightning Protection, ICLP 2004, Avignon, France, 2004.

[12] E.D. Sunde, Earth conduction effects in transmission systems, Dover, New York, 1968.